

# Orbital periods of cataclysmic variables identified by the SDSS. III. Time-series photometry obtained during the 2004/5 International Time Project on La Palma

M. Dillon<sup>1</sup>, B.T. Gänsicke<sup>1</sup>, A. Aungwerojwit<sup>2,1</sup>, P. Rodríguez-Gil<sup>3</sup>, T.R. Marsh<sup>1</sup>, S.C.C. Barros<sup>1</sup>, P. Szkody<sup>4</sup>, S. Brady<sup>5</sup>, T. Krajci<sup>6</sup>, A. Oksanen<sup>7</sup>

<sup>1</sup> *Department of Physics, University of Warwick, Coventry CV4 7AL, UK*

<sup>2</sup> *Department of Physics, Faculty of Science, Naresuan University, Phitsanulok, 65000, Thailand*

<sup>3</sup> *Instituto de Astrofísica de Canarias, 38200 La Laguna, Tenerife, Spain*

<sup>4</sup> *Astronomy Department, University of Washington, Seattle, WA98195, USA*

<sup>5</sup> *5 Melba Drive, Hudson, NH 03051, USA*

<sup>6</sup> *Astrokolkhoz Observatory, 1351 Cloudcroft, NM 88317, USA*

<sup>7</sup> *Hankasalmi Observatory, Kyllikinkatu 1, FI-40100 Jyväskylä, Finland*

Accepted 2008 Month day. Received 2008 Month day; in original form 2008 Month day

## ABSTRACT

We present time resolved CCD photometry of 15 cataclysmic variables (CVs) identified by the Sloan Digital Sky Survey (SDSS). The data were obtained as part of the 2004/05 International Time Programme on La Palma. We discuss the morphology of the light curves and the CV subtypes and give accurate orbital periods for 11 systems. Nine systems are found below the 2–3 h orbital period gap, of which five have periods within a few minutes of the  $\sim 80$  min minimum orbital period. One system each is found within and above the gap. This confirms the previously noted trend for a large fraction of short-period systems among the SDSS CVs. Objects of particular interest are SDSS J0901+4809 and SDSS J1250+6655 which are deeply eclipsing. SDSS J0854+3905 is a polar with an extremely modulated light curve, which is likely due to a mixture of cyclotron beaming and eclipses of the accretion region by the white dwarf. One out of five systems with white-dwarf dominated optical spectra exhibits non-radial pulsations.

**Key words:** binaries: close – binaries: eclipsing – binaries: spectroscopic – stars: dwarf novae – novae, cataclysmic variables – white dwarfs.

## 1 INTRODUCTION

Cataclysmic variables (CVs) contain white dwarfs accreting from (quasi) main-sequence stars. Because of their large number and the relatively simple nature of their stellar components, CVs hold a great potential to test and improve our understanding of compact binary evolution, in particular of orbital angular momentum loss and the impact of mass loss on the structure of the donor star. The severe disagreements between the predictions of the “standard” theory of CV evolution (e.g. Rappaport et al. 1983; Kolb 1993; Politano 1996; Howell et al. 2001) and the properties of the observed CV population (Patterson 1984; Gänsicke 2005) have stimulated a substantial number of alternative/additional theoretical approaches over the last two decades (e.g. Shara et al. 1986; Clemens et al. 1998; King et al. 2002; Schenker et al. 2002; Willems et al. 2005). However, at present a quantitative test of these efforts is unfeasible, as the  $\sim 650$  moderately well

studied CVs (Ritter & Kolb 2003) represent an inhomogeneous and incomplete population discovered by a number of different methods (e.g. Gänsicke 2005; Pretorius et al. 2007).

The Sloan Digital Sky Survey (SDSS; York et al. 2000) has the potential to dramatically improve the observational side of CV population studies. Sampling a large volume in *ugriz* colour space and extending deeper than any previous large-scale survey, SDSS provides the most homogeneous and complete sample of CVs to date. At the time of writing, the sample of definite SDSS CVs contains  $\sim 220$  systems, of which  $\sim 180$  are new discoveries (Szkody et al. 2002b, 2003, 2004, 2005, 2006, 2007a [henceforth PSI–PSVI] Roelofs et al. 2004; Anderson et al. 2005; Schmidt et al. 2007, Groot et al. 2007, submitted).

The newly identified CVs have been followed-up by a number of groups (e.g. Wolfe et al. 2003; Pretorius et al. 2004; Woudt & Warner 2004; Peters & Thorstensen 2005; Roelofs et al. 2005; Trampusch et al. 2005; Gänsicke et al.

2006; Southworth et al. 2006, 2007a,b; Littlefair et al. 2006a,b). Our group has been awarded the International Time 2004/5 on La Palma for the study of SDSS CVs, and we report in this paper photometric time series obtained for 15 systems. Spectroscopic observations of 15 systems will be reported in a second paper (Dillon et al. in prep), and a detailed discussion of the overall properties of the SDSS CV sample will be given in a third paper (Gänsicke et al. in prep). In Sect. 2, we provide a brief description of the instrumentation and data reduction used, and in Sect. 3 we outline the adopted time series analysis methods. Results on individual objects are presented in Sect. 4, and a general discussion of our results is given in Sect. 5.

## 2 OBSERVATIONS

The bulk of our differential CCD photometry was obtained using five different telescopes on La Palma as part of the 2004/5 International Time Programme, with some additional data obtained at Calar Alto and three small-aperture telescopes. We selected as targets for photometric observations primarily systems that were too faint for spectroscopy with the 2–4 m telescopes available on La Palma. A total of 15 SDSS CVs were observed, 12 of which on more than one occasion (Table 1). All data were reduced using the photometry pipeline described by Gänsicke et al. (2004). In brief, the images were bias and flat-field corrected in MIDAS, aperture photometry was performed using the **SExtractor** (Bertin & Arnouts 1996), and differential magnitudes were measured relative to a nearby comparison star. Differential magnitudes were then converted to apparent magnitudes using the  $g'$  magnitude of the comparison star obtained from the SDSS data base. While data obtained in the  $V$ -band can be calibrated using the colour transformations available on the SDSS web site, some systematic uncertainty on the apparent magnitudes of the systems observed in white light or with a non-standard filter remains. Below we provide a brief description of the instrumentation used at the different telescopes.

**Isaac Newton Telescope (INT).** The Wide Field Camera (WFC) is an optical mosaic camera used at the prime focus of the 2.5 m INT. It consists of four  $2048 \times 4100$  pixel EEV CCDs with a  $0.33''\text{pixel}^{-1}$  scale. Binning and windowing is not supported and hence all four full CCD frames have to be read out, which causes a dead-time of 42 s between two exposures.

**William Herschel Telescope (WHT).** The Auxiliary Port Imaging Camera (AUX Port) is mounted at the Cassegrain auxiliary port of the 4.2 m WHT. It is equipped with a  $1024 \times 1024$  pixel TEK CCD with a  $0.11''\text{pixel}^{-1}$  scale and provides an unvignetted field of view of  $\sim 1.8'$ . We used the AUX Port with a binning  $4 \times 4$ , decreasing the read-out time of the full CCD to a few seconds.

**Liverpool Telescope (LT).** The LT is a fully robotic 2 m telescope. The optical CCD camera RATCAM is equipped with a  $2048 \times 2048$  pixel EEV with  $0.14''\text{pixel}^{-1}$  scale covering a field of view of  $4.6' \times 4.6'$ . A binning  $2 \times 2$  is the default for this instrument. Windowing is not supported, and the read-out time for the full CCD is 10 s.

**Nordic Optical Telescope (NOT).** The low resolution imaging spectrograph ALFOSC on the 2.5 m NOT

telescope contains a  $2048 \times 2048$  pixel EEV CCD with an  $0.19''\text{pixel}^{-1}$  scale. The data were obtained binning the CCD  $2 \times 2$  and windowing closely around the target star, reducing the read-out time to a few seconds.

**Telescopio Nazionale Galileo (TNG).** The Device Optimized for the Low Resolution (DOLORES) on the 3.6 m TNG uses a  $2048 \times 2048$  pixel Loral CCD with a  $0.28''\text{pixel}^{-1}$  scale, covering a field of view of about  $9.4' \times 9.4'$ . The CCD was not binned but windowed in order to reduce the readout time to  $\sim 10$  s.

**Calar Alto (CA22).** The Calar Alto Faint Object Spectrograph (CAFOS) was used on the 2.2 m telescope. The instrument is equipped with a  $2048 \times 2048$  pixel SITE CCD with a scale of  $0.53''\text{pixel}^{-1}$  and a field of view of  $16'$ . Windowing was applied to reduce the readout time to  $\sim 10$  s.

**Hankasalmi Observatory (HaO).** We used a RCOS Carbon 16RC0.40 m Ritchey-Chretien telescope mounted on a Paramount ME, along with an SBIG STL-1001E CCD camera. The data were dark subtracted and flat fielded. Aperture photometry was then performed with the MaxImDL software.

**Astrokolkhoz Observatory (AO).** We used a 0.28 m Schmidt-Cassegrain telescope with a focal length of 1.8 m along with an SBIG ST-7 CCD camera binned  $2 \times 2$ . The data were dark and bias subtracted and flat fielded and measured using aperture photometry using AIP4WIN.

**Hudson Observatory (HO).** Observations were made from a private observatory located in southern New Hampshire, USA. Instruments include a 0.4 m robotic Newtonian Telescope mounted on a Paramount ME along with an SBIG ST-8XME CCD camera, and BVRI filters (which were not utilised due to the faint magnitude). The robotic system was programmed to monitor a list of poorly studied CV candidates and to initiate immediate time-series observations if an outburst is detected, as was the case with SDSS J090103.93+480911.1 and SDSS J125023.84+665526.4. All images were bias subtracted, flat-field corrected and photometrically reduced using MaxIm DL.

Sample light curves for each object are shown in Fig. 1, where we also display the SDSS identification spectra from PSI-V for convenience. At a first visual inspection, the light curves of the observed systems display a wide variety of morphologies, including apparently non-periodic flickering (SDSS J0018+3454), deep eclipses (SDSS J1250+6655, SDSS J0901+4809), periodic double-humps (e.g. SDSS J0151+1400), double-peaked flare-like events (SDSS J0854+3905), or absence of significant variability altogether (SDSS J1514+4549, SDSS J0904+4402). The light curves obtained on different nights for an individual system are rather similar in all cases, except for SDSS J0901+4801, SDSS J1250+6655 and SDSS J2116+1134, which were observed both in quiescence and in outburst.

## 3 TIME SERIES ANALYSIS

All light curves were analysed using several methods provided by the MIDAS/TSA context. More specifically, we computed periodograms based on Scargle's (1982) method

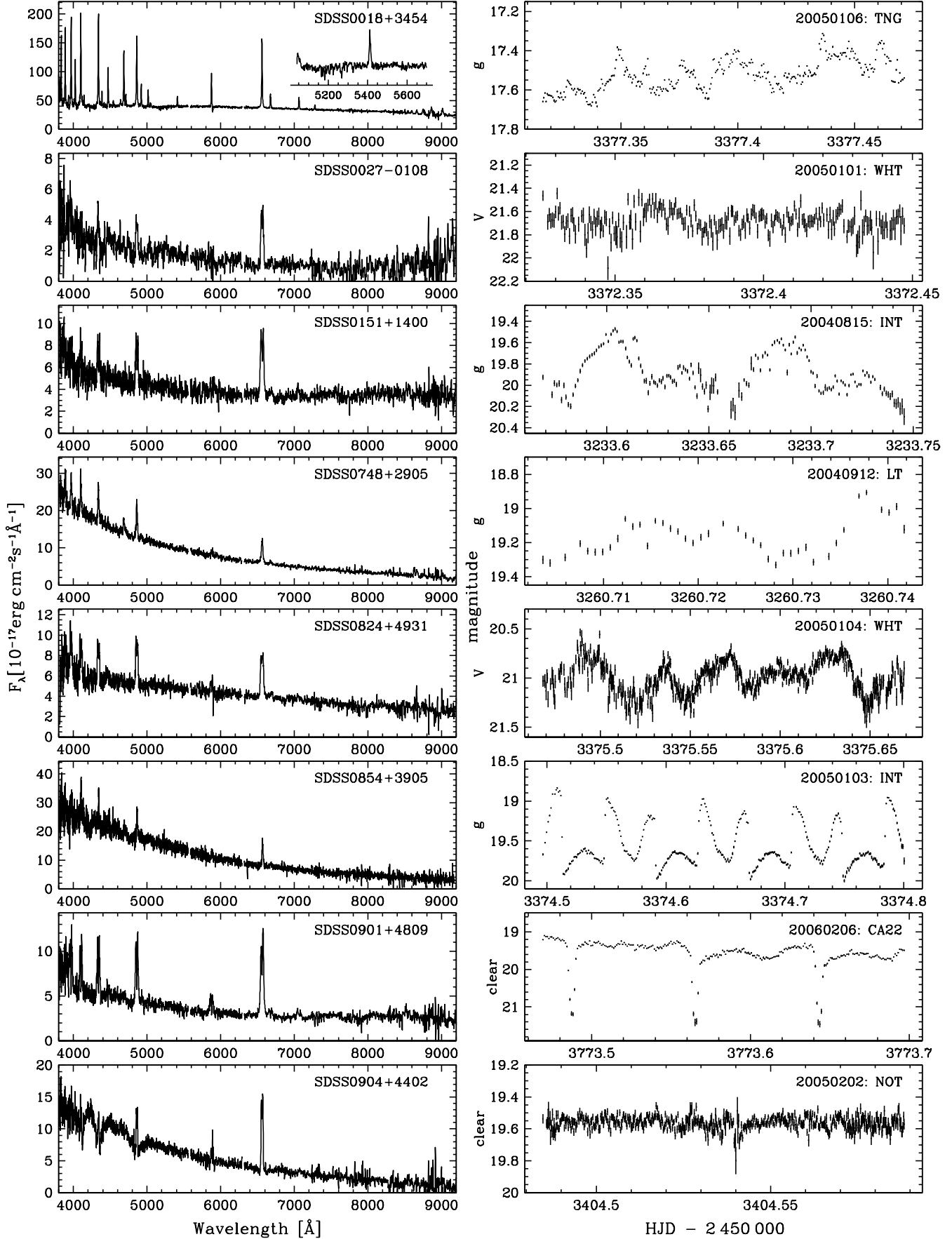
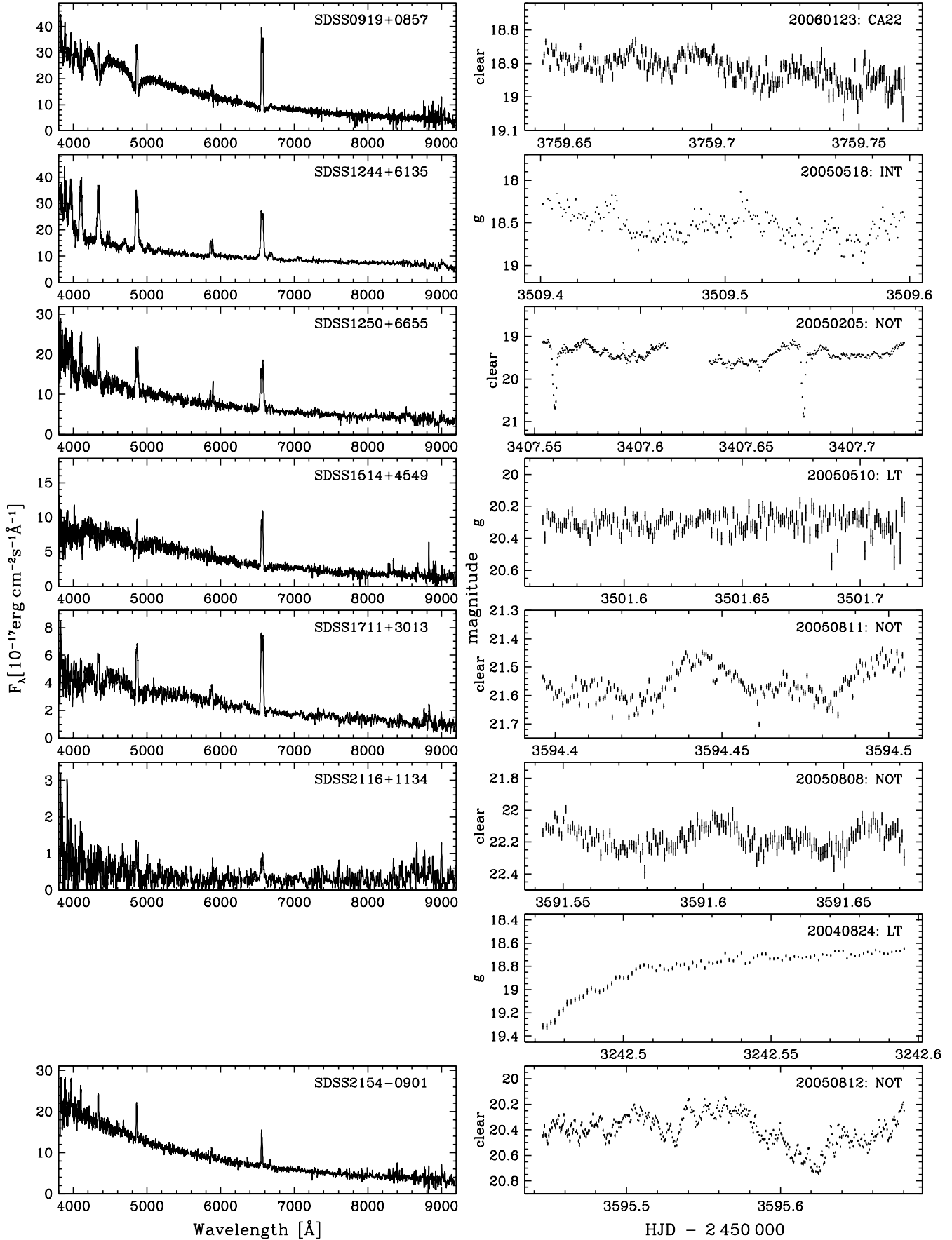


Figure 1. Sample light curves for all objects observed (Table 1) along with their SDSS identification spectra from PSI-V.



**Table 1.** Log of observations and summary of the system properties. We list the orbital periods as determined from our photometric time series, the  $g$  magnitude from the SDSS imaging data, the magnitude during our observations, information on the system type (WD = white-dwarf dominated spectrum, RD = secondary star visible, He II = noticeable He II emission line, EC = eclipsing, DN = dwarf nova, AM = polar), the date of the observation, the telescope and filter used, the exposure time, the number of images, and a reference to the identification paper.

SDSSJ	$P_{\text{orb}}$ [min]	$g_{\text{SDSS}}$	mag	Type	Date/Time [UT]	Telescope	Filter	Exp(s)	Frames	Source
001856.93+345444.3	-	17.8	17.2	He II/RD	2005-01-01 20:55-23:46	INT	clear	25	153	PSIV
			17.8		2005-01-05 19:50-23:01	TNG	clear	40	176	
			17.5		2005-01-06 19:35-23:17	TNG	clear	30	321	
			17.7		2005-01-07 19:29-22:48	TNG	clear	30	275	
002728.01-010828.5	$85.44 \pm 0.07$	20.7	20.6	DN/WD	2004-12-31 20:08-22:55	WHT	V	40-100	215	PSIV
			20.6		2005-01-01 19:49-22:44	WHT	V	40	233	
			20.6		2005-01-02 19:35-22:29	WHT	V	40	231	
			19.9		2004-08-15 02:47-05:39	INT	$g$	40	129	
015151.87+140047.2	$118.68 \pm 0.04$	20.3	19.9	DN/RD	2004-08-16 01:35-05:50	INT	$g$	40-60	169	PSI
			19.9		2004-08-17 01:58-05:30	INT	$g$	40-60	148	
			19.2		2004-09-12 04:57-05:53	LT	$g$	60	50	
074813.54+290509.2	-	18.6	19.2	He II	2004-09-12 04:57-05:53	LT	$g$	60	50	PSIII
082409.73+493124.4	$95 \pm 3$	19.3	21.0	DN	2005-01-04 23:06-03:56	WHT	V	20	698	PSI
			20.8		2005-01-05 21:00-04:56	WHT	V	30	380	
			21.0		2005-01-07 00:37-04:24	WHT	V	20-30	532	
			19.2		2005-01-03 00:07-07:13	INT	$g$	80-120	112	
085414.02+390537.3	$113.26 \pm 0.03$	19.2	19.5	AM	2005-01-03 23:47-07:13	INT	$g$	50-60	303	PSIV
			19.9		2006-02-06 23:08-04:27	CA22	clear	60	240	
			16.2		2007-10-06 06:52-09:39	HO	clear	160	52	
090103.93+480911.1	$112.14793 \pm 0.00005$	19.9	17.0	DN/RD/EC	2007-10-09 08:38-12:12	AO	clear	60	192	PSIV
			17.1		2007-10-09 20:42-00:22	HaO	clear	95	128	
			18.1		2007-10-11 08:10-12:09	AO	clear	90	138	
			19.4		2005-01-05 02:33-04:06	INT	$g$	30-40	73	
			19.1		2005-01-05 04:10-06:55	INT	clear	30-35	143	
091945.11+085710.0	$81.6 \pm 1.2$	19.9	19.6	WD	2005-02-02 23:30-02:00	NOT	clear	15	544	PSIV
			18.9		2006-01-24 03:17-06:14	CA22	clear	25	252	
			18.8		2005-05-18 21:37-02:20	INT	$g$	40-60	215	
124426.26+613514.6	$142.9 \pm 0.2$	18.8	18.6	He II	2005-05-19 21:03-00:29	INT	$g$	40	160	PSIII
			18.7		2005-05-20 21:02-00:05	INT	$g$	40-60	123	
			18.7		2005-02-03 04:19-05:38	NOT	clear	15-30	151	
			19.3		2005-02-05 01:14-05:19	NOT	clear	10-20	451	
125023.85+665525.5	$84.5793893 \pm 0.0000036$	18.7	19.0	DN/EC	2005-03-16 03:15-06:42	LT	$g$	60	169	PSII
			19.1		2005-03-17 23:19-23:47	LT	$g$	60	33	
			19.0		2005-03-18 01:13-03:14	LT	$g$	60	166	
			16.0		2008-01-29 01:36-08:52	HO	clear	70	306	
			16.4		2008-01-31 01:18-10:40	HO	clear	120	231	
			16.6		2008-02-04 03:32-08:06	HO	clear	160	93	
			20.1		2005-04-01 04:11-06:29	LT	$g$	60	114	
			20.1		2005-05-10 01:30-05:35	LT	$g$	60	205	
151413.72+454911.9	-	19.7	20.2	WD	2004-08-14 21:15-01:03	INT	$g$	40-60	141	PSIII
			20.2		2004-08-15 21:05-00:13	INT	$g$	40-60	129	
			20.2		2004-08-16 21:05-23:46	INT	$g$	45-120	63	
			20.3		2005-08-11 21:28-00:04	NOT	clear	40	198	
211605.43+113407.5	$80.2 \pm 2.2$	15.3	20.3	DN	2005-08-12 21:11-22:30	NOT	clear	40	101	PSIII
			22.1		2005-08-09 00:54-03:59	NOT	clear	60	164	
			22.1		2005-08-10 00:40-02:24	NOT	clear	60	93	
			22.1		2005-08-11 02:40-04:33	NOT	clear	90	70	
			18.8		2005-08-24 23:12-02:08	LT	$g$	90	110	
215411.12-090121.6	$319 \pm 0.7$	19.2	20.4		2005-08-11 00:29-05:42	NOT	W	40	396	PSII
			20.3		2005-08-12 22:33-04:11	NOT	W	40	427	
			20.4		2005-08-14 00:33-05:38	NOT	W	40	376	

clear = white light, V = Johnson-V band,  $g$  = Sloan  $g$ -band, W = broad-band red cut-off.

(**scargle**), as well as on Schwarzenberg-Czerny's (1982) analysis-of-variance (**aov**), and Schwarzenberg-Czerny's (1996) extension of **aov** which fits the phase-folded data with orthogonal trigonometric polynomials (**ort**). Fourier-type methods such as **scargle** work best on light curves with smooth, quasi-sinusoidal variations, but are not well-

suited for the analysis of light curves with sharp features, such as eclipses, where **aov** and **ort** are preferred. A noticeable feature of **aov** and **ort** periodograms is substantial power at sub-harmonics of the strongest signal.

We calculated periodograms using all three methods for each individual light curve, as well as for each system com-

binning all available data. All light curves had their nightly mean subtracted before the analysis. In 11 systems the time series analysis revealed the presence of a periodic signal in the photometric data. We interpret these signals as the orbital periods of the systems. The periodograms calculated for those objects from their combined data sets are shown in Fig. 2, along with phase-folded light curves. In order to assess the likelihood that the strongest alias represents the true orbital period we applied a test based on bootstrapping simulations (see Press et al. 1992, chapter 15.6), following the approach described in Southworth et al. (2006, 2007b). The probabilities determined from this bootstrapping procedure are slightly on the pessimistic side, as each simulation is using only a subset of the entire available data.

For the eclipsing systems SDSS J0901+4809 and SDSS J1250+6655 the above methods were carried out for completeness. However, more accurate orbital periods can be determined from the analysis of the mid-eclipse times. In order to measure those times (Table 2) we plotted the original light curve with a copy mirrored in time, and shifted the copy until the bottom of the eclipse in both light curves showed the closest agreement. Orbital ephemerides were then determined from linear fits to the mid-eclipse times.

The periods and errors reported in Table 1 were determined from sine fits near the best-choice aliases in the periodograms (Fig. 2), except for SDSS J0901+4809 and SDSS J1250+6655, where the periods and errors were determined from linear ephemeris fits to the mid-eclipse timings reported in Table 2.

#### 4 RESULTS ON INDIVIDUAL SYSTEMS

In this Section, we present the results of our photometric observations and discuss our findings for each individual system. A more generic discussion of these results follows in Sect. 5.

**SDSS J0018+3454.** The SDSS identification spectrum in Fig. 1 displays strong narrow emission lines. While the strength of  $\text{He II } \lambda 4686$  is suggestive of a magnetic CV nature, the absence of noticeable polarisation ( $< 0.2\%$ ) argues against SDSS J0018+3454 being a polar (PSIV). Time-series spectroscopy with  $3 \text{ \AA}$  resolution obtained over a 2 h failed to detect a significant radial velocity variation (PSIV). Our photometry obtained over four nights shows non-periodic flickering activity with an amplitude of  $\sim 0.1 \text{ mag}$  on time scales of  $\sim 20 - 40 \text{ min}$  and night-to-night variations of  $\sim 0.3 \text{ mag}$ . Close inspection of the SDSS spectrum of SDSS J0018+3454 reveals a broad absorption dip centred on  $5150 \text{ \AA}$ , along with a host of narrow absorption lines in that range (see insert in Fig. 1), typical of a mid-K main sequence star, strongly suggesting an early-type donor star. In fact, the continuum spectrum of SDSS J0018+3454 resembles closely that of SDSS J204448.92-045928.8, for which Peters & Thorstensen (2005) determined a donor star spectral type of K4-5 and an orbital period of 2419 min. The contribution of the donor star in SDSS J0018+3454 is weaker than in SDSS J2044-0459, indicating a relatively larger contribution of the accretion luminosity in SDSS J0018+3454. Combining the spectroscopic appearance with the absence of noticeable radial velocity variations over short time scales (PSIV), it appears likely that SDSS J0018+3454 is a long-

**Table 2.** Eclipse timings, cycle number, and the difference in observed minus computed eclipse times using the ephemerides in Eqs. (1) and (2).

Object	$T_0$ (HJD)	$O - C$ (s)	Cycle
SDSS J0901+4801	2453773.48757	4	0
	2453773.56532	-7	1
	2453773.64332	4	2
	2454379.78725	-1	7785
	2454379.86519	4	7786
	2454382.90215	-28	7825
	2454382.98060	21	7826
	2454383.36973	-2	7831
	2454383.44766	2	7832
	2454384.84940	-8	7850
SDSS J1250+6655	2454384.92749	11	7851
	2453407.55964	-1	0
	2453407.67713	1	2
	2453445.67918	5	649
	2453445.73774	-10	650
	2453447.49997	4	680
	2453447.55857	-9	681
	2453447.61750	9	682
	2454494.58109	6	18507
	2454494.63971	-4	18508
	2454494.69853	3	18509
	2454494.75714	-8	18510
	2454494.81597	1	18511
	2454496.57856	46	18541
	2454496.63684	7	18542
	2454496.69558	7	18543
	2454496.75419	-4	18544
	2454496.81320	20	18545
	2454496.93046	1	18547
	2454500.68934	-17	18611
	2454500.74828	2	18612

period CV, and phase-resolved spectroscopy spanning a sufficiently long time should easily provide the radial velocity variation of the donor star from its absorption lines. The strong  $\text{He II } \lambda 4686$  emission line in a presumably long-period system is very untypical, and unravelling the nature of this object should be high-priority task.

**SDSSJ 0027-0108 (EN Cet).** This object has been identified as a dwarf nova in outburst and spectroscopically confirmed as a cataclysmic variable by Esamdin et al. (1997). The SDSS spectrum of EN Cet (Fig. 1, PSIV) is of rather poor quality, containing a double-peaked  $\text{H}\alpha$  emission line. The observed flux upturn at the red end of the spectrum is interesting, as it could represent the donor star in this object. However, it appears more likely that it is an artifact from the night sky calibration, which is problematic in fibre spectroscopy at such low flux levels. An *ort* analysis of our *V*-band photometry obtained over three consecutive nights reveals a periodic signal at  $16.9 \text{ d}^{-1}$  (85.4 min) and contains power at the second harmonic as well. A bootstrap simulation (Sect. 3) suggests a  $\sim 73\%$  probability for the choice of the strongest alias in the periodogram corresponding to the intrinsic period of the data, the flanking  $1 \text{ d}^{-1}$  aliases have likelihoods of  $\sim 10\%$ . Phase-folding the data using this period results in a light curve with a double-hump morphology (Fig. 2). Such a light curve shape is observed in a number of ultrashort-period CVs, such

as e.g. WZ Sge (Patterson et al. 1998), RZ Leo, BC UMa, MM Hya, & HV Vir (Patterson et al. 2003), WX Cet (Mennickent 1994; Rogoziecki & Schwarzenberg-Czerny 2001), or HS 2331+3905 (Araujo-Betancor et al. 2005)), and we interpret the 85.4 min signal as the orbital period of the system. From a sine-fit to the data, we determine  $P_{\text{orb}} = 85.44 \pm 0.07$  min.

**SDSS J0151+1400.** The SDSS spectrum (Fig. 1, PSI) contains double-peaked Balmer emission lines, suggesting a moderately high inclination. The He I lines are very weak, and the slope of the spectrum has a break near 6500 Å, suggesting that the secondary star may contribute to the observed flux in the red part of the SDSS spectrum. To explore this possibility, we have applied a three-component model consisting of a blackbody (to represent the blue continuum), an isothermal/isobaric hydrogen slab (Gänsicke et al. 1999, to represent the accretion disc), and an M-star template (Rebassa-Mansergas et al. 2007, to represent the secondary star). A reasonable fit to the SDSS spectrum of SDSS J0151+1400 is achieved for a blackbody temperature of 8500 K, and a radius of the blue component of  $1.4 \times 10^9$  cm, a slab temperature and column density of 5800 K and  $2 \times 10^{-2}$  g cm $^{-2}$ , and a spectral type of the donor of M6, with all three components scaled to a distance of 480 pc (see Gänsicke et al. 2006; Rodríguez-Gil et al. 2005; Southworth et al. 2006 for more details on this type of spectral modelling). These parameters should be considered with some caution, as the SDSS spectrum is of rather poor quality and covers an unknown orbital phase. Nevertheless, the spectral type suggested by our fit is consistent with the donor stars that are typically observed in this orbital period range (e.g. Silber et al. 1994; Remillard et al. 1994; Mennickent & Diaz 2002). The geometric extension and temperature of the blue continuum component, combined with the absence of broad Balmer absorption lines, argues against an origin on the white dwarf but rather for an origin from the accretion disc edge and/or bright spot. A single outburst of SDSS J0151+1400 has been detected by Hiroyuki Maehara in January 2007 (vsnet-alert 9139).

The  $g$ -band light curves obtained on three consecutive nights display a double-humped morphology with an amplitude of  $\sim 0.3$  mag. The strongest signal in an *ort* periodogram is detected at a frequency of  $12.1 \text{ d}^{-1}$  (118.8 min), with some power at the second harmonic. A bootstrap simulation shows that the alias choice is unambiguous for SDSS J0151+1400. In analogy to SDSS 0027-0108, we interpret the strongest signal as the orbital period of the system, and obtain from a sine-fit to the data  $P_{\text{orb}} = 118.68 \pm 0.04$  min.

**SDSS J0748+2905.** While the identification spectrum displays He II emission (Fig. 1, PSIII) the absence of noticeable polarisation ruled out a polar nature for this object (PSIII). An orbital period of 2.5 h was estimated by PSIII from radial velocity variations, though, this must be considered a rough estimate only as the system was observed only for  $\simeq 2.6$  h. Our single  $g$ -band light curve covering  $\sim 1$  h shows variability on time scales of 15–20 min with an amplitude of  $\simeq 0.2$  mag. We found the system at a mean magnitude of  $g \simeq 19.2$ , whereas the light curve in PSIII showed the system at  $V \simeq 18.3$ , indicating long-term variability of the object (the nearby companion unresolved in the photometry

reported in PSIII has  $g = 22.5$  and can safely be neglected). No coherent periodicity was detected in our data.

**SDSS J0824+4931.** The SDSS spectrum of SDSS J0824+4931 (Fig. 1, PSI) broadly resembles that of SDSS J0027-0108 and SDSS J0151+1400 with slightly double-peaked Balmer emission lines along with very weak He I lines. The secondary star does not noticeably contribute at red wavelengths. Our  $V$ -band light curves are of a double-humped shape with a  $\sim 0.5$  mag amplitude. We observed SDSS J0824+4931 on three consecutive nights (Table 1), with very poor conditions in the second night. During our observations, SDSS J0824+4931 was substantially fainter than the magnitude reported from the SDSS imaging data. Using only the data from the first and the third night, an *ort* analysis results in an unambiguous signal at  $15.16 \text{ d}^{-1}$  (2), and a sine-fit to the data gives  $P_{\text{orb}} = 94.99 \pm 0.02$  min. In contrast, an *ort* analysis of the combined data from all three nights (not shown) gives three possible frequencies:  $14.67 \text{ d}^{-1}$  (98.1 min),  $15.16 \text{ d}^{-1}$  (95.0 min), and  $15.65 \text{ d}^{-1}$  (92.0 min). These three signals have roughly equal strength in the power spectrum, and similar probabilities in a bootstrap simulation.

Boyd et al. (2007) recently performed the first photometric study of SDSS J0824+4931 during a superoutburst, detecting superhumps with a period of  $100.14 \pm 0.07$  min and an underlying weak signal at  $98.9 \pm 0.9$  min, which they interpreted as the orbital period of the system, suggesting a superhump excess of  $\epsilon = 0.13$ . Using the superhump period from Boyd et al. (2007), our three possible orbital period aliases, 98.1 min, 95.0 min, and 92.0 min, result in  $\epsilon = 0.021, 0.054, 0.088$ , respectively. Based on Patterson's (2005) compilation of known superhump excesses, the 98.1 min alias seems most probably, as it implies a low, but not unusual superhump excess, similar to e.g. KV And (Patterson et al. 2003) and HS 0417+7445 (Aungwerojwit et al. 2006). The 95.0 min the 98.1 min periods seem less likely and implausible, as no dwarf novae with  $\epsilon > 0.05$  are found below the period gap (e.g. Nogami et al. 2001; Patterson et al. 2003, 2005).

In summary, as the exact value of the orbital period of SDSS J0824+4931 remains somewhat debatable we prefer to err on the conservative side, and report in Table 1 an error including the two flanking aliases from our photometry, hence  $P_{\text{orb}} = 95 \pm 3$  min.

**SDSS J0854+3905 (EUVE J0854+390).** This system was identified as a possible magnetic CV by Christian et al. (2001). Their optical spectra displayed large radial velocity variations suggesting a period of  $< 0.2$  d. The SDSS spectrum (Fig. 1, PSIV) shows the system fainter by a factor  $\sim 10$  with much weaker He II emission. Spectropolarimetric observations of SDSS J0854+3905 confirm the magnetic nature of the system, displaying circular polarisation levels of up to  $-30\%$  with cyclotron harmonic humps clearly visible in the spectrum (PSIV).

Our two  $g$ -band light curves of SDSS J0854+3905 show a strong periodic double-peaked flare-like morphology with a peak-to-peak amplitude of  $\sim 1$  mag with a period of  $\sim 2$  h. An *ort* periodogram calculated from our data gives an unambiguous signal at  $12.7 \text{ d}^{-1}$  (113 min), and a sine-fit (including four harmonics because of the sharply modulated light curve morphology) results in  $P_{\text{orb}} = 113.26 \pm 0.03$  min.

The extreme shape of the modulation can be under-

stood in terms of a combination of cyclotron beaming from the accretion column near the white dwarf and the accretion region being eclipsed by the white dwarf for parts of the spin cycle, similar to the geometry in AM Her (Gänsicke et al. 2001). Maximum flux occurs near the orbital phases  $\varphi \simeq 0.26$  and  $\varphi \simeq 0.68$  (Fig. 2, where the zero-point of the phase is arbitrary), where the line-of-sight must be closest to being perpendicular to the magnetic field lines in the accretion column. The sharp rise and drop in flux observed near phases  $\phi \simeq 0.2$  and  $\phi \simeq 0.75$  recurs with high precision in both nights, and suggests that the accretion column/region is self-eclipsed by the body of the white dwarf. The drop in flux centred on  $\phi \simeq 0.5$  occurs when the magnetic pole rotates into view, and the angle between the line-of-sight and the magnetic field lines in the accretion region reaches a minimum value. The modulation observed between  $\phi \simeq 0.75 - 0.20$  could be related to accretion onto the second pole, or a geometric projection effect of the accretion stream. Given that the white dwarf spin in polars is magnetically locked to the orbital period, we deduce  $P_{\text{orb}} = 113.26$  min. SDSS J0854+3905 appears to be a promising object for (spectro)polarimetric follow-up observations, which will allow a precise reconstruction of the accretion geometry.

**SDSS J0901+4809.** The SDSS spectrum (Fig. 1, PSII) shows deep central absorption structures in the Balmer and He I emission lines, suggesting a high inclination of the system. The slope of the spectrum displays a break near 6500 Å, similar to SDSS J0151+1400. Applying the same type of three-component model as for SDSS J0151+1400, we find that rather similar parameters provide a satisfactory fit to the SDSS spectrum of SDSS J0901+4809, i.e. a blackbody temperature and radius of 9500 K and  $1.2 \times 10^9$  cm, respectively, a slab temperature and column density of 6100 K and  $2 \times 10^{-2}$  g cm $^{-2}$ , respectively, and a donor star spectral type of M6, all scaled to a distance of 520 pc. All in all, SDSS J0151+1400 and SDSS J0901+4809 seem to be very similar in their parameters with the latter one having a slightly higher inclination.

Our single filterless light curve of SDSS J0901+4809 (Table 1) identifies the system as deeply eclipsing one. On 6 Oct 2007, one of us (SB) detected the first outburst of SDSS J0901+4809, finding the object at an unfiltered magnitude of  $\sim 16.2$ . Over the course of 5 days, it faded to an unfiltered magnitude of  $\sim 18.1$ , after which it was too faint for the equipment available at that time. We measured the eclipse centres by mirroring eclipse profiles and shifting them in time until the best overlap was achieved. The eclipse timings are reported in Table 2. A linear fit to the three eclipse times results in the eclipse ephemeris

$$T_0(\text{HJD}) = 2\,453\,773.48752(3) + 0.077880505(35) \times E \quad (1)$$

i.e. an orbital period of 112.15 min (12.84 d $^{-1}$ ). The corresponding cycle numbers and observed-minus-computed (O-C) eclipse times are reported in Table 2. There is a small chance for a cycle miscount, which would result in a somewhat shorter period of 0.077870588(50) d (112.13 min), however, the O-C values prefer the period given in Eq. 1. SDSS J0901+4809 is a prime candidate for high time resolution eclipse studies to measure accurate binary parameters (see e.g. Feline et al. 2004; Littlefair et al. 2006a).

**SDSS J0904+4402.** The identification spectrum of

SDSS J0904+4402 (Fig. 1, PSIII) shows that the white dwarf is the dominant source of light in this system. No trace of the donor star is detected in the red part of the spectrum. Mildly double-peaked Balmer emission lines are superimposed on the broad absorption lines from the white dwarf. Our *g*-band and filterless photometry of SDSS J0904+4402 does not contain any periodicity that could be identified as the orbital period.

Inspired by the identification of a number of accreting white dwarfs among the SDSS CVs which exhibit non-radial pulsations (Woudt & Warner 2004; Warner & Woudt 2004; Gänsicke et al. 2006; Nilsson et al. 2006), we have inspected the periodogram of SDSS J0904+4402 for the presence of short-period signals. The INT *g*-band data contain a (by means of a Monte-Carlo simulation) significant signal at 8.678(34) min (165.94(65)d $^{-1}$ ) with an amplitude of 26 mmag. The NOT data contain two significant signals at 7.678(40) min (187.53(99)d $^{-1}$ ) and 12.16(11) min (118.8(1.1)d $^{-1}$ ), with amplitudes of 12.5 mmag and 11.3 mmag, respectively. However, given the fact that the two runs yield different periods, we would consider SDSS J0904+4402 only as a pulsating WD candidate, as accretion-related flickering could easily mimic such a putative pulsation signal. Additional time-series photometry is encouraged to test whether or not the periods detected at the INT and NOT are detected again.

**SDSS J0919+5028.** The SDSS spectrum of SDSS J0919+5028 (Fig. 1, PSIV) is dominated by the white dwarf with no signature from the donor star. PSIV estimated  $P_{\text{orb}} \simeq 1.4$  h from 2 h of time-resolved spectroscopy, and compared the system to GW Lib, the first ZZ Ceti star found in a CV (van Zyl et al. 2000).

Our single filterless light curve shows humps with a period of  $\sim 40$  min superimposed on a downward trend in the system brightness. We detrended the overall trend by subtracting from the light curve a copy of the data smoothed with an 80-point box car. An *ort* periodogram computed from the detrended light curve contains broad peaks centred at a frequency of 17.7 d $^{-1}$  and its harmonic, suggesting that the actual morphology of the light curve is double-humped, similar to SDSS J0027-0108, SDSS J0151+1400, and SDSS J0824+4931. A sine-fit to the data results in  $P_{\text{orb}} = 81.6 \pm 1.2$  min.

The power spectrum at shorter periods reveals a marginally significant signal at  $259.93 \pm 0.94$  s (332.41 d $^{-1}$ ), which we interpreted as a possible non-radial pulsation mode. Based on the detection of that signal in additional data, Mukadam et al. (2007) confirmed SDSS J0919+5028 as a white dwarf pulsator.

**SDSS J1244+6135.** The SDSS spectrum (Fig. 1, PSII) displays strong double-peaked Balmer and He I emission lines, suggesting a high inclination. Our *g*-band data obtained over three consecutive nights reveal a periodic modulation with an amplitude of  $\simeq 0.2$  mag. A *scargle* periodogram contains a cluster of aliases with the strongest signal at 10.0 d $^{-1}$  (144 min). The absence of power at the second harmonic indicates that the light curve morphology of SDSS J1244+6135 is not, as in e.g. SDSS J0027-0108 or SDSS J0151+1400, double-humped. A bootstrap simulation shows that the alias choice is unambiguous with a likelihood of 97.2%. We interpret the observed modulation as the orbital period, and determine  $P_{\text{orb}} = 142.9 \pm 0.2$  min.



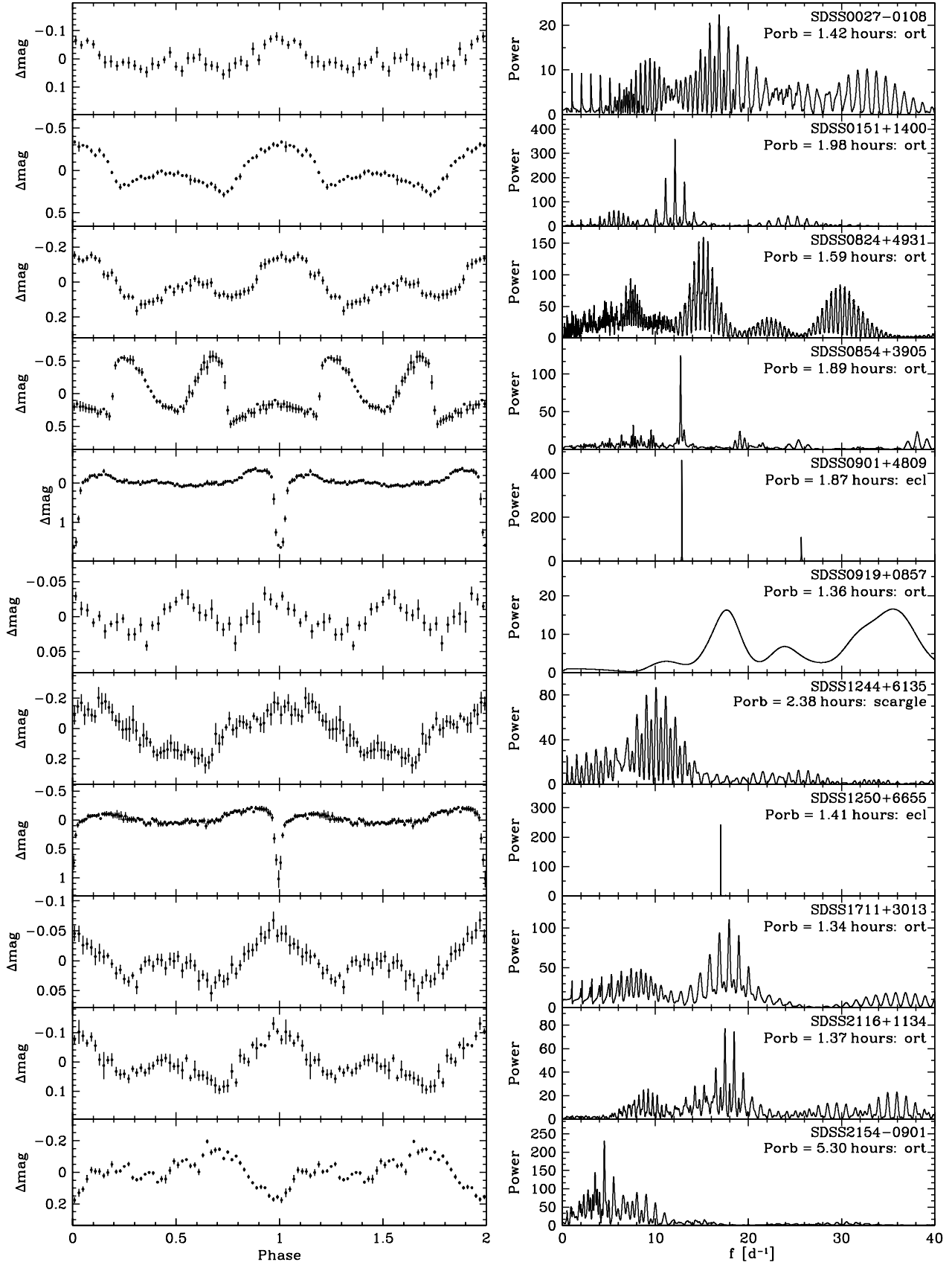


**Figure 2.** Periodograms (right panels) and phase-folded light curves (left panels) of the 11 SDSS CVs for which we could determine an orbital period from our photometry (Table 1). The method indicated to compute the individual periodograms (*scargle*, *aov*, *ort*) is indicated (see Sect. 3).

**SDSS J1250+6655.** The identification spectrum of SDSS J1250+6655 (Fig. 1, PSII) contains broad double-peaked Balmer emission lines with deep central absorption, typical of high-inclination systems. No spectroscopic feature from the donor star is detected in the red part of the spectrum. PSII suggested an orbital period of 5.6 h on the basis of a short (2.3 h) set of time-resolved spectroscopy, but the long (15 min) integration times could not resolve eclipses. Our NOT light curve of SDSS J1250+6655 revealed the occurrence of deep ( $\sim 2$  mag) eclipses. A first outburst of this CV was detected by one of us (SB) on 29 January 2008. The mid-eclipse times (Table 2) were determined from all our light curves in an analogous way as for SDSS J0901+4809, and a linear fit to those times gives the following eclipse ephemeris

$$T_0(\text{HJD}) = 24\,534\,07.55966(7) + 0.0587356870(43) \times E, \quad (2)$$

i.e. an orbital period of  $84.5793893(63)$  min ( $\simeq 17.0\text{d}^{-1}$ ). With SDSS J1250+6655 being close to the orbital minimum period, eclipse studies appear especially worthwhile to determine accurate masses and radii for the stellar components in this system – lying between the eclipsing XZ Eri ( $P_{\text{orb}} = 88.0$  min,  $M_2 = 0.0842 \pm 0.0024 M_{\odot}$ , Feline et al. 2004) and SDSS J1035+0551 ( $P_{\text{orb}} = 82.1$  min,  $M_2 = 0.052 \pm 0.002 M_{\odot}$ , Littlefair et al. 2006b; Southworth et al. 2006).

**SDSS J1514+4549.** This is another white dwarf dominated CV, with no noticeable contribution from the donor star (Fig. 1, PSIV). The two  $g$ -band light curves reveal very little variability, and no periodicity that could be ascribed to the orbital period is detected in the periodograms calculated from the data. Our two observations found the object at a constant mean brightness of  $g \simeq 20.2$ . Nilsson et al. (2006) reported the detection of non-radial pulsations with a period of 559.3 s in two observations, and the absence of this signal in a third observation. The non-detection of this period in our two observing runs suggests that SDSS J1514+4559, if it is a pulsator, has a rather unstable pulsation spectrum.

**SDSS J1711+3013.** Very similar to SDSS J1514+4549, the SDSS spectrum of SDSS J1711+3013 clearly reveals the white dwarf (Fig. 1, PSIII) but no evidence for the secondary star. We obtained a total of 5 light curves on three consecutive nights in August 2004 and on two consecutive nights in August 2005. All light curves reveal a double-humped morphology. An *ort* periodogram of the 2005 data, which is of better quality than the 2004 data, contains the strongest peak at  $17.9\text{d}^{-1}$  (80.4 min), which we interpret as the orbital period. A bootstrap simulation shows that the choice of this alias is unambiguous (99.6% likelihood). A sine-fit to the data results in  $P_{\text{orb}} = 80.35 \pm 0.05$  min. Combining the data from both years confirms this result, but does not allow a more accurate period determination as the periodogram suffers from strong 1-year aliases. We note that no significant signal at shorter periods is found in any of our observations, with a detection limit of 12 mmag, which is consistent with the non-detection of ZZ Ceti pulsations in this object by Mukadam et al. (2007)

**SDSS J2116+1134.** The SDSS spectrum of SDSS J2116+1134 (Fig. 1, PSIII) shows double-peaked Balmer emission lines on a very weak continuum. The object was found in the SDSS imaging data at  $g = 15.3$ ,

whereas we measured  $g = 21.8$  from the SDSS spectrum, clearly showing that SDSS J2116+1134 is a dwarf nova. In August 2004, we obtained photometry with the LT and found the object rising in magnitude from  $g = 19.4$  to 18.6 over the course of a 3 h-long observing run, indicating another outburst of the system. In August 2005, filterless photometry obtained over three consecutive nights showed the system at a mean magnitude of  $g \simeq 22.2$ , displaying a double-humped light curve. An *ort* periodogram contains two strong aliases at  $17.5\text{d}^{-1}$  (82.3 min) and  $18.5\text{d}^{-1}$  (77.8 min), with the bootstrap test giving a 2/3 preference for the lower frequency alias. Sine fits to both aliases determine the two periods to  $\pm 0.03$  min, however, given the ambiguous choice of the correct alias, we adopt  $P_{\text{orb}} = 80.2 \pm 2.2$  min as a conservative value.

**SDSS J2154-0901.** The identification spectrum of SDSS J2154-0901 (Fig. 1, PSII) shows a blue continuum superimposed by relatively weak and narrow Balmer and He I lines, as well as weak He II  $\lambda 4686$ . Our light curves of SDSS J2154-0901 obtained over three consecutive nights show substantial flickering activity and a long term modulation with a broad minimum and a steep decline. An *ort* periodogram contains a strong signal at  $4.5\text{d}^{-1}$  (320 min), and a sine fit to the data gives  $P_{\text{orb}} = 319 \pm 0.7$  min. SDSS J2154-0901 is the only system above the 2–3 h period gap among the 11 systems for which we were able to determine periods.

## 5 DISCUSSION

Substantial effort has gone into calculating models of the intrinsic population of galactic CVs (e.g. de Kool 1992; Kolb 1993; Politano 1996; Howell et al. 2001), however, comparison with the observed properties of the known CV sample consistently failed to match the predicted orbital period distribution, the total space density of CVs, and the expected tight correlation between orbital period and mass transfer rate (e.g. Patterson 1984; Ringwald 1993; Gänsicke 2005). While these discrepancies may be partially related to shortcomings in the theories of common envelope evolution and orbital angular momentum loss, it is clear that the heterogeneous set of known CVs (Ritter & Kolb 2003) is not well-suited for a quantitative test of the population models.

SDSS is currently establishing the largest, deepest ( $g \sim 20$ ), and most homogeneous sample of CVs, with an estimated  $\sim 300$  CVs by the end of the SDSS operations. Establishing the detailed properties of this CV sample is a major task. Our photometric study of 15 CVs contained within the SDSS spectroscopic data base has led to the determination of the orbital periods for 11 of them, along with additional information on CV subtypes. This underlines the potential of time-series photometry on mid-size aperture telescopes for measuring the orbital periods of the faint SDSS CVs.

Inspecting the distribution of orbital periods among the 11 CVs studied here (Table 1), it becomes apparent that nine systems have periods below the 2–3 h period gap, one within the gap, and only one above the gap. We were unable to determine the orbital periods for four systems, but based on their spectroscopic appearance the white-dwarf dominated SDSS J0904+4402 and SDSS J1514+4549 are likely to have periods below the gap, and SDSS J0748+2905 and SDSS J0018+3454 are likely to have periods above the

gap. Our result corroborates the findings of Szkody et al. (2003, 2007a) and Southworth et al. (2006, 2007b), who noticed a larger fraction of short-period systems among the SDSS CVs compared to the previously known CVs (see e.g. Aungwerojwit et al. 2006 for CVs from the Hamburg Quasar Survey or Pretorius et al. 2007 for CVs from the Palomar Green Survey). In particular, five systems have periods within  $\sim 5$  min of the  $\sim 80$  min orbital minimum. Three of those have optical spectra dominated by the white dwarf (SDSS J0027–0108, SDSS J0919+0857, and SDSS J1711+3013), with no signature from the mass donor, indicating both very low mass transfer rates and a very late spectral type of the companion star. All three closely resemble SDSS J1035+0551, an eclipsing white-dwarf dominated CV (Southworth et al. 2006) with an low-mass brown dwarf donor (Littlefair et al. 2006b). About  $\sim 20\%$  of the CVs identified by SDSS have white-dwarf dominated spectra (PSI–VI) similar to SDSS J1035+0551 and the systems studied here, and orbital period measurements are available for  $\sim 20$  of these systems, with the majority being found near the minimum period (e.g. Woudt & Warner 2004; Pretorius et al. 2004; Zharikov et al. 2006; Gänsicke et al. 2006; Southworth et al. 2006, 2007b). Hence, it appears likely that complete follow-up of the SDSS CV sample will lead to a substantial increase of CVs with extremely short orbital periods.

A final note concerns the detection of non-radial pulsations in a number of SDSS CVs (Woudt & Warner 2004; Gänsicke et al. 2006; Nilsson et al. 2006; Mukadam et al. 2007). While all of the confirmed pulsators have white-dwarf dominated spectra, it does not appear possible to predict the presence of pulsations in a given system just on the base of its optical spectrum. Among the CVs studied here, five exhibit the white dwarf in the SDSS spectrum, but only one system appears to be a non-radial pulsator (SDSS J0919+0857). Ultraviolet observations show that pulsations can appear over a wide range of white dwarf effective temperatures (Szkody et al. 2002a; Araujo-Betancor et al. 2005; Szkody et al. 2007b), and hence the “instability strip” is apparently less well-defined than for single white dwarfs (Mukadam et al. 2004; Gianninas et al. 2006). This difference may be related to the contamination of the envelope by accreted helium in the CV white dwarfs (Arras et al. 2006).

## 6 CONCLUSIONS

We have obtained time-series photometry for 15 CVs contained in the SDSS spectroscopic data base. Periodic variability detected in 11 of these systems allowed us to establish their orbital periods. We find that 9 systems are located below the 2 – 3 h orbital period gap, one within the gap, and one above, confirming that the SDSS CV sample contains a larger fraction of short-period systems compared to the previously known CVs. Two of the new CVs are eclipsing, SDSS J0901+4809 and SDSS J1250+6655, and are prime targets for detailed binary parameter studies. One polar, SDSS J0854+3905, exhibits a sharply modulated light curve and warrants polarimetric follow-up in order to establish the accretion geometry. Finally, only one out of five CVs having white-dwarf dominated spectra displays non-radial pulsations.

## ACKNOWLEDGEMENTS

MD was supported by an STFC Studentship. AA thanks the Royal Thai government for generous funding. PS acknowledges some support from NSF grant AST 02-05875. SCCB is supported by FCT. Based in part on observations made with the William Herschel Telescope and the Isaac Newton Telescope, which are operated on the island of La Palma by the Isaac Newton Group in the Spanish Observatorio del Roque de los Muchachos (ORM) of the Instituto de Astrofísica de Canarias (IAC); on observations made with the Telescopio Nazionale Galileo operated on the island of La Palma by the Centro Galileo Galilei of the INAF (Istituto Nazionale di Astrofisica) at the ORM of the IAC; on observations made with the Nordic Optical Telescope, operated on the island of La Palma jointly by Denmark, Finland, Iceland, Norway, and Sweden, in the ORM of the IAC; The Liverpool Telescope is operated on the island of La Palma by Liverpool John Moores University at the ORM of the IAC. The WHT, INT, NOT, TNG, and LT data were obtained as part of the 2004 International Time Programme of the night-time telescopes at the European Northern Observatory.

## REFERENCES

- Anderson, S. F., et al., 2005, *AJ*, 130, 2230
- Araujo-Betancor, S., et al., 2005, *A&A*, 430, 629
- Arras, P., Townsley, D. M., Bildsten, L., 2006, *ApJ Lett.*, 643, L119
- Aungwerojwit, A., et al., 2006, *A&A*, 455, 659
- Bertin, E., Arnouts, S., 1996, *A&AS*, 117, 393
- Boyd, D., Shears, J., Koff, R., 2007, *Journal of the British Astronomical Association*, in press, (arXiv:0707.1865)
- Christian, D. J., Craig, N., Dupuis, J., Roberts, B., 2001, *Informational Bulletin on Variable Stars*, 5032, 1
- Clemens, J. C., Reid, I. N., Gizis, J. E., O’Brien, M. S., 1998, *ApJ*, 496, 352
- de Kool, M., 1992, *A&A*, 261, 188
- Esamdin, A., Dong, X., Zhao, Y., 1997, *IAU Circ.*, 6763
- Feline, W. J., Dhillon, V. S., Marsh, T. R., Brinkworth, C. S., 2004, *MNRAS*, 355, 1
- Gänsicke, B. T., 2005, in Hameury, J.-M., Lasota, J.-P., eds., *The Astrophysics of Cataclysmic Variables and Related Objects*, ASP Conf. Ser. 330, p. 3
- Gänsicke, B. T., Sion, E. M., Beuermann, K., Fabian, D., Cheng, F. H., Krautter, J., 1999, *A&A*, 347, 178
- Gänsicke, B. T., Fischer, A., Silvotti, R., de Martino, D., 2001, *A&A*, 372, 557
- Gänsicke, B. T., Araujo-Betancor, S., Hagen, H.-J., Harlaftis, E. T., Kitsionas, S., Dreizler, S., Engels, D., 2004, *A&A*, 418, 265
- Gänsicke, B. T., et al., 2006, *MNRAS*, 365, 969
- Gianninas, A., Bergeron, P., Fontaine, G., 2006, *AJ*, 132, 831
- Howell, S. B., Nelson, L. A., Rappaport, S., 2001, *ApJ*, 550, 897
- King, A. R., Schenker, K., Hameury, J. M., 2002, *MNRAS*, 335, 513
- Kolb, U., 1993, *A&A*, 271, 149
- Littlefair, S. P., Dhillon, V. S., Marsh, T. R., Gänsicke, B. T., 2006a, *MNRAS*, 371, 1435

- Littlefair, S. P., Dhillion, V. S., Marsh, T. R., Gänsicke, B. T., Southworth, J., Watson, C. A., 2006b, *Science*, 314, 1578
- Mennickent, R., 1994, *A&A*, 285, 979
- Mennickent, R. E., Díaz, M. P., 2002, *MNRAS*, 336, 767
- Mukadam, A. S., Winget, D. E., von Hippel, T., Montgomery, M. H., Kepler, S. O., Costa, A. F. M., 2004, *ApJ*, 612, 1052
- Mukadam, A. S., Gänsicke, B. T., Szkody, P., Aungwerojwit, A., Howell, S. B., Fraser, O. J., Silvestri, N. M., 2007, *ApJ*, 667, 433
- Nilsson, R., Uthas, H., Ytre-Eide, M., Solheim, J.-E., Warner, B., 2006, *MNRAS*, 370, L56
- Nogami, D., Kato, T., Baba, H., Novák, R., Lockley, J. J., Somers, M., 2001, *MNRAS*, 322, 79
- Patterson, J., 1984, *ApJS*, 54, 443
- Patterson, J., Richman, H., Kemp, J., Mukai, K., 1998, *PASP*, 110, 403
- Patterson, J., et al., 2003, *PASP*, 115, 1308
- Patterson, J., et al., 2005, *PASP*, 117, 1204
- Peters, C. S., Thorstensen, J. R., 2005, *PASP*, 117, 1386
- Politano, M., 1996, *ApJ*, 465, 338
- Press, W., Teukolsky, S., Vetterling, W., Flannery, B., 1992, *Numerical Recipes in FORTRAN 77*, Cambridge Univ. Press, Cambridge
- Pretorius, M. L., Woudt, P. A., Warner, B., Bolt, G., Patterson, J., Armstrong, E., 2004, *MNRAS*, 352, 1056
- Pretorius, M. L., Knigge, C., Kolb, U., 2007, *MNRAS*, 374, 1495
- Rappaport, S., Joss, P. C., Verbunt, F., 1983, *ApJ*, 275, 713
- Rebassa-Mansergas, A., Gänsicke, B. T., Rodríguez-Gil, P., Schreiber, M. R., Koester, D., 2007, *MNRAS*, 382, 1377
- Remillard, R. A., Schachter, J. F., Silber, A. D., Slane, P., 1994, *ApJ*, 426, 288
- Ringwald, F., 1993, *The Cataclysmic Variables from the Palomar-Green Survey*, Ph.D. thesis, Dartmouth College
- Ritter, H., Kolb, U., 2003, *A&A*, 404, 301
- Rodríguez-Gil, P., Gänsicke, B. T., Hagen, H.-J., Marsh, T. R., Harlaftis, E., Kitsionas, S., Engels, D., 2005, *A&A*, 431, 269
- Roelofs, G. H. A., Groot, P. J., Steeghs, D., Nelemans, G., 2004, in *Tovmassian, G., Sion, E., eds., Compact Binaries and Beyond*, no. 20 in Conf. Ser., RMAA, p. 254
- Roelofs, G. H. A., Groot, P. J., Marsh, T. R., Steeghs, D., Barros, S. C. C., Nelemans, G., 2005, *MNRAS*, 361, 487
- Rogoziecki, P., Schwarzenberg-Czerny, A., 2001, *MNRAS*, 323, 850
- Scargle, J. D., 1982, *ApJ*, 263, 835
- Schenker, K., King, A. R., Kolb, U., Wynn, G. A., Zhang, Z., 2002, *MNRAS*, 337, 1105
- Schmidt, G. D., Szkody, P., Henden, A., Anderson, S. F., Lamb, D. Q., Margon, B., Schneider, D. P., 2007, *ApJ*, 654, 521
- Schwarzenberg-Czerny, A., 1989, *MNRAS*, 241, 153
- Schwarzenberg-Czerny, A., 1996, *ApJ Lett.*, 460, L107
- Shara, M. M., Livio, M., Moffat, A. F. J., Orio, M., 1986, *ApJ*, 311, 163
- Silber, A. D., Remillard, R. A., Horne, K., Bradt, H. V., 1994, *ApJ*, 424, 955
- Southworth, J., Gänsicke, B. T., Marsh, T. R., de Martino, D., Hakala, P., Littlefair, S., Rodríguez-Gil, P., Szkody, P., 2006, *MNRAS*, 373, 687
- Southworth, J., Gänsicke, B. T., Marsh, T. R., de Martino, D., Aungwerojwit, A., 2007a, *MNRAS*, 378, 635
- Southworth, J., Marsh, T. R., Gänsicke, B. T., Aungwerojwit, A., Hakala, P., de Martino, D., Lehto, H., 2007b, *MNRAS*, 382, 1145
- Szkody, P., Gänsicke, B. T., Howell, S. B., Sion, E. M., 2002a, *ApJ Lett.*, 575, L79
- Szkody, P., et al., 2002b, *AJ*, 123, 430
- Szkody, P., et al., 2003, *AJ*, 126, 1499
- Szkody, P., et al., 2004, *AJ*, 128, 1882
- Szkody, P., et al., 2005, *AJ*, 129, 2386
- Szkody, P., et al., 2006, *AJ*, 131, 973
- Szkody, P., et al., 2007a, *AJ*, 134, 185
- Szkody, P., et al., 2007b, *ApJ*, 658, 1188
- Tramposch, J., Homer, L., Szkody, P., Henden, A., Silvestri, N. M., Yirak, K., Fraser, O. J., Brinkmann, J., 2005, *PASP*, 117, 262
- van Zyl, L., Warner, B., O'Donoghue, D., Sullivan, D., Pritchard, J., Kemp, J., 2000, *Baltic Astronomy*, 9, 231
- Warner, B., Woudt, P., 2004, in *Kurtz, D. W., Pollard, K. R., eds., Variable Stars in the Local Group*, ASP Conf. Ser. 310, p. 392
- Willems, B., Kolb, U., Sandquist, E. L., Taam, R. E., Dubus, G., 2005, *ApJ*, 635, 1263
- Wolfe, M. A., Szkody, P., Fraser, O. J., Homer, L., Skinner, S., Silvestri, N. M., 2003, *PASP*, 115, 1118
- Woudt, P. A., Warner, B., 2004, *MNRAS*, 348, 599
- York, D. G., et al., 2000, *AJ*, 120, 1579
- Zharikov, S. V., Tovmassian, G. H., Napiwotzki, R., Michel, R., Neustroev, V., 2006, *A&A*, 449, 645

This paper has been typeset from a  $\text{\LaTeX}$  file prepared by the author.